MINISTRY OF SUPPLY

AERONAUTICAL RESEARCH COUNCIL
REPORTS AND MEMORANDA

An Experimental Investigation of the Effect of Engine Loads on Wing Structures

By

J. L. REDDAWAY, B.A.

An Experimental Investigation
of the Effect of Engine Loads on Wing Structures

By

J. L. Reddaway, B.A.

Communicated by the Director General of Scientific Research. (Air),
Ministry of Supply

Reports and Memoranda No. 3062*

April, 1950

Summary.—Three cellulose-nitrate model wings, identical except for rib flexibility, have been tested under conditions reproducing typical engine loads. Stress distributions have been found experimentally by means of electrical resistance strain-gauges. The distribution due to an abrupt change of torsion has been compared with a theory by Williams, and that due to an abrupt change of shear with a theory by Taylor.

Local stresses at the engine nacelle are found to be appreciably higher in practice than would have been predicted by either of these theories. The discrepancies, moreover, are found to increase with rib flexibility.

---

1. *Introduction.*—The practice of designing wings with overhanging engines leads to the application of concentrated loads to the wing structure at the engine nacelles.

The premature failure of two wing specimens just outboard of an engine nacelle, whilst undergoing static strength tests, has drawn attention to strains induced by such concentrations. In neither case would the theoretical increases in stress, above that predicted by the normal engineers' theory of bending, due to abrupt changes of torsion as dealt with by Williams[1] or due to abrupt changes of shear as dealt with by Taylor[2], have accounted for the failures. Williams's theory is based on an assumption of closely spaced rigid ribs and that of Taylor on the assumption that the additional stress due to an abrupt change of shear is uniform across sections of the wing.

The present investigation, using cellulose-nitrate models, was made to check whether these assumptions are tenable when endeavouring to calculate the stress distribution.

2. *Description of Tests.*—2.1. *The Specimens.*—Three cellulose-nitrate models were made reproducing the essential characteristics of a semi-span wing, with light spars and heavy stringers. They were identical except for the rib construction and were basically rectangular boxes, without taper, three feet long and with cross-sections six inches by two inches.

The ribs, at two-inch pitch, were of three types. The first model employed ribs $\frac{1}{8}$-in. thick with large central cut-outs, representing ribs which would be suitable for the insertion of fuel tanks. They were connected to the front and rear spars of the box and to the undersides of the stringers. There was no attachment directly to the top or bottom skin. The ribs of the second model differed in that they were without the central cut-outs and only 0·040-in. thick, the method of attachment remaining the same. Ribs as for the second model (without central cut-outs and 0·040-in. thick) were used for the third model but with a further difference from the first in that the ribs were extended to reach the top and bottom skins of the box. Slots were provided in the ribs, for the stringers to pass through, and the ribs were cemented all around their periphery so that there was a sealed bulkhead between each rib bay. A $\frac{1}{16}$-in. diameter hole was drilled in each rib to equalise the air pressures inside and outside the model.

---

* R.A.E. Report Struct. 64, received 18th August, 1950.

Initially, each model incorporated at one section a single plain sheet of cellulose nitrate to represent an engine nacelle and to act as a loading frame. Subsequent modifications were made to this loading frame to find the influence of the method of attachment of the nacelle to the wing on the strain distribution.

The boxes were all built in at the root using a wooden plug inside and an outer fitted case, also of wood. The tip ribs were a quarter of an inch thick and considered stiff.

The material used in the construction of the models was a thermoplastic of the nitro-cellulose type.

Fig. 1 shows the general arrangement and details of the specimens, the different types of rib being shown in Fig. 2. A photograph of two of the models is included as Fig. 3.

2.2 *Loading Conditions and Test Cases.*—The loading conditions at the engine nacelle were as follows:

Case No. 1.—A down load, on an engine frame consisting of a single plain sheet of cellulose nitrate $\frac{1}{4}$-in. thick affixed to the bottom skin, front spar, and one-sixth of the top surface of the model, at a rib section 14 in. from the root. The load was applied well forward of the front spar.

Case No. 2.—A repeat test of Case 1 with the loading frame slit so that load was applied to the front spar only (*see* Fig. 1).

Case No. 3.—A down load at the front spar and an equivalent up load at the rear spar producing an abrupt change of torque at the loading section (It should be noted that this also produces local abrupt changes of shear on each spar).

Case No. 4.—Equal up loads at both front and rear spars giving an abrupt change of shear at the loading section.

The details of the initial loading frame, as used under Case 1, together with the amendments incorporated for subsequent tests, are shown in Fig. 1.

Preliminary tests showed that, not only was there a considerable change in Young's modulus of the model material due to temperature and humidity changes, but that there were even local variations in a model itself. To overcome this difficulty the following procedure was adopted. After each test load had been applied, and removed, and before atmospheric conditions had time to alter appreciably, strain-gauge readings were again taken with a single up-load applied to the wing tip. Thus, each case was accompanied with a 'calibration test' with a single tip load. The analysis is based on the comparative strain-gauge results of the two sets of readings without direct reference to the Young's modulus of the material. The ratio of Young's modulus to the Shear modulus is still required for the theoretical analysis and this has been taken as 3, giving a value of 0·5 for Poisson's ratio.

The absolute values of the loads applied were determined by the strength of the model. The ratio of the tip load to engine load was such that the ratio of the bending moment at the engine nacelle due to the tip load, to the torque applied at the loading frame, was approximately the same as that on a full-scale test where a wing failure had occurred. The tip load was 20 lb, giving a bending moment of $20 \times 22 = 440/lb$ in. at the nacelle, and the engine load under Case 1 was 10 lb, giving a torque of 106·2 lb/in. at the centre-line of the box, *i.e.*, a ratio of 4·15 to compare with the full-scale test figures of B.M. $= 14·30 \times 10^6$ lb/in. and torque $3·02 \times 10^6$ with a ratio of 4·74.

It was convenient, in most cases, to increase the engine load to give greater strain-gauge deflections and, thus, greater accuracy. The results were reduced to give the equivalent strain measurement under a torque of 106·2 lb/in. before any analysis was carried out.

2.3. *Strain Measurements.*—The strain was measured with electrical resistance strain-gauges. 200-ohm self-adhesive gauges were attached by embedding them in a solution of cellulose nitrate

dissolved in acetone. The gauge length was $\frac{1}{2}$ in. and the gauge factor (ratio of fractional change of resistance to change of strain) 2·2. Direct strains only were measured throughout.

The usual dummy system[4] employing strips of the model material for mounting the dummy gauges individually was not used. Three models were used for the investigation and only one was tested at a time. Thus it was possible, by matching the resistance of corresponding gauges on all the models, to use either of the two models not being tested as a complete dummy specimen to provide temperature and humidity compensation for the one under test.

Measurements were made at 36 positions giving the variation in strain along the corners of the boxes and across two or three sections. Fig. 4 is a key to the gauge positions.

2.4. *Measurement of Rib Stiffness.*—Dial gauges were attached to the corners of each model, at the first rib outboard of the engine loading frame, to show the relative rotation of the rear spar to the bottom surface of the box. This gives a measure of the change in shape of the cross-section under torque and, hence, an indication of the relative rib stiffness between the models.

3. *Results.*—Mean values of the measurement of rib stiffnesses are given in Table 1. This table gives the relative rotation of the rear spar to the bottom surface, at the first rib outboard of the loading section (a distance from the loading section equal to the spar depth), on all models under the three torsional loading cases.

No attempt has been made to deduce actual strains in the models. As noted above the strains, under each loading case, are tabulated as a proportion of the strains produced by a load at the tip. In the analysis the following procedure is adopted:

Cases 1, 2 and 3.—(a) Results from these cases have been reduced to give the equivalent strain-gauge readings for a total torque of 106·2 lb/in., *i.e.*, the torque as produced by a load of 10 lb on the engine frame as originally built (The actual loads applied are given in Table 1).

(b) For a gauge a distance y inboard of the engine mounting frame and a distance x from the model tip we have strain-gauge readings of A units under a load W_1 applied at the tip and B units (*i.e.*, the equivalent value as found in (a)) under a load W_2 on the overhanging engine frame. This reading of B units is due not only to pure torsion applied at the loading frame but also to the bending effect of the engine load when considered as acting at the flexural centre. In order to compare the experimental results with Williams's theory, which deals with the stresses induced under pure torsion, a correction is needed for this bending effect.

Thus an overall bending moment W_1x at the section through the gauge position due to the tip load gives a reading of A units and therefore a load W_2 on the engine mounting frame producing a bending moment of W_2y at the same section will give a reading of $\{A(W_2y/W_1x)\}$ units due to bending alone.

The gauge reading due to the torsional effect will therefore be $\{B - (W_2y/W_1x)A\}$.

This correction to the B reading applies only to gauges inboard of the loading section.

(c) These corrected values (*i.e.*, B units outboard of the engine loading frame or $\{B - (W_2y/W_1x)A\}$ inboard of the loading frame) have been divided by the readings given by the wing tip load acting alone (*i.e.*, A units). The results have been noted as percentage concentrations. Thus the term 'concentration' as used here denotes the local increase of stress above that found from the simple engineers' theory of bending.

Case 4.—An identical procedure with that used for the other cases has been adopted but in this case the results were first reduced to give the equivalent readings for an abrupt change of shear of 10 lb.

Table 2 lists the percentage concentrations at each gauge position under all four loading cases. It should be noted that the gauge positions on the first model differ from those on the other two and the results cannot be compared directly.

3

The theoretical concentrations on the line of the gauges, along the edges of the box, have been calculated by Williams's method using the assumption of stiff ribs and the application of a pure torque at the loading section. With these assumptions the theoretical concentrations are the same under the first three loading cases and for all three models. These theoretical concentrations have been plotted in Figs. 5, 6 and 7. Fig. 5 incorporates the experimental results from all three models under loading Case 1 and Fig. 7 the results, again from all three models, under loading Case 3. Fig. 6 includes plots of points obtained by an addition of the experimental results obtained in loading Cases 1 and 4. The presence of the slits in the engine loading frame for loading Case 2 weakened the models considerably and it was not advisable to load the model with more than 10 or 15 lb, even when strengthening fillets had been provided on the front spar. Concentrations from this case have only been quoted for the two sections adjacent to the loading frame, for at other sections the readings are comparable with the amount of strain-gauge drift and are therefore not very reliable. This case has not been plotted in a similar fashion to the other two.

For the fourth case the theoretical concentrations due to a single abrupt change of shear have been estimated using Taylor's theory, assuming that the additional stress due to an abrupt change of shear is uniform across sections of the wing. Fig. 8 shows curves of theoretical concentrations compared with experimental results along the four edges of the boxes for all three models.

Figs. 9, 10 and 11 give pictures of the strain distribution on sections across the top and bottom surfaces of the models. The concentrations, under all loading conditions, calculated from the readings of the gauges on sections A, B and C (see Fig. 4) have been plotted on a separate figure for each model. Each figure shows the variation between the four loading cases.

4. *Discussion of Results.*—Except for the ribs the models were identical so that all differences in results, other than experimental variation, must be attributed to the change in rib stiffness which, although probably small in itself nevertheless plays an important part in deciding the strain distribution.

Note that theoretically the concentrations or reliefs on the top and bottom skins of the models are the same. Experimentally this is not so and this fact gives an appearance of scatter to the plots of the strain-gauge results. A close examination of the points on either the upper or lower surface of the spars (they can be distinguished readily from the convention used in plotting) reveals a fairly consistent pattern.

More attention is paid to the results obtained outboard of the loading section, for these have suffered no preliminary adjustments (*see* section 3(*b*)) such as have been made to the gauge readings inboard.

4.1. *Rib Stiffness.*—The following points emerge from the study of the relative rotation of the rear spar to the bottom surface on all models under the three torsional loading cases (*see* Table 1):

(*a*) Case 1 gives a false picture of the shape-retaining properties of the ribs as the loading frame itself acts as a heavy stiffener in the vicinity of the section where the measurements were made.

(*b*) There is an apparent low rib stiffness of Model 3 under loading Case 2; this result is considered to be wrong and has been ignored*.

(*c*) The method of attachment of the ribs to the skin is of greater importance in retaining the cross-sectional shape than the method of construction of the rib itself. The Case 3 results show that there is little difference between Models 1 and 2, with ribs attached only indirectly to the

---

* NOTE: The results from this loading case were more liable to error as the dial gauge readings were rather small, particularly for the rear spar, due to the strength limitation on the load which could be applied. This is not altogether a satisfactory position but the attachment of a different loading frame, for use in Case 3, did not allow a further check to be made.

4

skins through the stringers, although the ribs themselves are quite different. Both models undergo considerable distortion whilst Model 3 completely retains its shape. Under this case the relative rotations of the rear spar to the bottom surface for Models 1 and 2, at the first rib outboard of the loading section, were 0·82 and 0·85 respectively. This corresponds to a shear angle of 0·16 deg in the worst case. Due to this similarity of Models 1 and 2 they have, in general, been referred to collectively, in the discussion that follows, as 'flexible rib' models. Furthermore, the use of the term rib stiffness, or rib flexibility, implies the ability, or inability, of the rib with its attachment to the skin to maintain the shape of the cross-section when under load.

4.2. *Pure Shear Effects* (*Case* 4).—A theory due to Taylor, on the stresses in built-up beams due to an abrupt change of shear at the loading section, has been used to compare with the experimental results. The section constants have been calculated treating each model as a box beam. The theory is really intended for spars and we should not expect too close an agreement with our results. A study of Figs. 8, 9, 10 and 11 reveals:

(*a*) Models 1 and 2 show an increase in stress concentration over the stiff rib model, of the order of 50 per cent, close to the loaded section.

(*b*) The theoretical peak stress concentration, on the spars, is of the same order as that found experimentally but the calculated rate of die away, along the spars, is much greater.

(*c*) The experimental results show that for each model at any section the stress concentration is a maximum at the spars dying away rapidly, with reversal of sign (giving a relief of stress), towards the centre of the section. The relief, in the centre, is of the order of 20 to 50 per cent of the concentrations at the spars.

(*d*) The theoretical values obtained at the first two sections outboard of the loading frame are an approximation to the mean stress concentration across the top and bottom skins, although, as noted under (*c*), the experimental values differ a great deal from the mean.

4.3. *Pure Torque Effects* (*Case* 3).—The following points are noted from Figs. 7, 9, 10, 11.

(*a*) There are marked differences between the first two models, with ribs attached to the skin only through the stringers, and the stiff-rib model:

(i) Stress concentrations on the front spar, and stress reliefs on the rear spar, adjacent to the loading frame, are of the order of 100 per cent greater than on the stiff-rib model.

(ii) For the flexible-rib models the die away outboard of the loading frame is such that there is a reversal in sign of the stress concentration towards the tip. This is not the case for the stiff-rib model (No. 3) where the concentrations die away exponentially to zero.

(*b*) Comparisons with the theoretical solution due to Williams shows that:

(i) for the stiff-rib model, close to the loading section, experimental results are slightly greater than the theoretical (order of 20 to 30 per cent). The concentrations or reliefs, depending on whether we examine the front or rear spars, fall rapidly to below the theoretical values as the distance from the engine frame is increased. This peculiarity is supported by a previous experimental investigation carried out by Williams and Smith[3] on a tube constructed of spruce and birch ply. For convenience a figure of Ref. 3 has been included here as Fig. 12. The curve gives the bending moments induced in the spars of a tube under an applied torsion at an intermediate section. The bending moments are not referred to the direct bending moments, which would obtain under tip loads, to give concentrations such as have been calculated in this note. The general pattern of the curve is, nevertheless, the same as given by the present tests.

(ii) for the flexible-rib models concentrations or reliefs are of the order of 100 to 150 per cent greater, at sections close to the loading frame, than those predicted by theory. Furthermore, the die-away factor is not, now, a simple exponential as the stress concentrations and reliefs fall to zero in approximately a distance equal to twice the spar depth and then change sign, although outboard of this point they are not of a high order.

5

(c) It should be pointed out that the torque was not applied in a ' Batho ' distribution to the loading section, i.e., equal up and down loads were applied to the front and rear spars whilst the ' Batho ' theory assumes, not only equal up and down loads on the front and rear spars (smaller than actually applied), but also equal fore and aft loads on the top and bottom skins so as to apply a uniform shear per inch to the whole section. This was also the case in the previous experimental investigation. Now this results in local abrupt changes of shear at the spars greater than would have been the case with a ' Batho ' distribution of loading. Consequently, although there is no overall abrupt change of shear on the model, it would be expected that similar effects to those produced under the Pure Shear Case (No. 4) would occur near the loading section. That this is so is borne out by a study of Figs. 9 to 11, which give the stress distribution across sections of the models, for they reveal that the stress distribution is not linear across the top and bottom skins at the first section outboard of the loading frame, but is peaked at the spars, where the load is applied, dying away in an exponential manner towards the centre of the section. At a distance equal to the spar depth away from the loaded section, i.e., at the second section investigated outboard of the loading frame, the distribution, within the limits of experimental accuracy, is linear as would be expected under pure torque. These remarks must be borne in mind when interpreting the facts noted under (a) and (b) above.

4.4. *Combined Loading Effects (Case 1).*—Fig. 5 gives a picture of the results obtained for all models under loading Case 1, i.e., an overhanging engine load on a stiff frame. The following points are noted:

(a) On all models the stress concentrations are greater on the front spar than the reliefs on the rear spar.

(b) In the case of the first two models (with flexible ribs) the concentrations on the front spar can be as much as 70 per cent greater than that predicted at the loading section assuming (i) stiff ribs and (ii) that the concentration is due solely to the bending stresses induced by torsion.

(c) For the third, and stiff-rib, model the concentrations on the front spar only exceed the theoretical by approximately 20 per cent at the first section outboard of the loading section.

Comment (a) can be explained fairly readily, for the effect of torsion is to give concentrations on the front spar and reliefs on the rear spar whilst the abrupt change of shear leads to concentrations on both front and rear spars.

Assuming then that the concentrations found experimentally are due not only to the torsion applied but also to the abrupt change of shear, a better comparison with theory can be made than given in Fig. 5. The results from loading Case 4 are due to a total upward load of 10 lb and the results from Case 1 are due to a downward load of 10 lb plus a torsional load. Adding the values of the concentrations obtained under these two cases gives an estimate of the concentrations to be expected under pure torsion, and it is these results which should be compared with the theoretical curves. Too good an agreement should not be expected for the method of dispersion of the change of shear into the structure is different. The comparison has been made in Fig. 6 and we see that the correspondence is much improved in that the results from front and rear spars are similar and closer to the theoretical solution. We note, too, that the mean of the concentrations and reliefs on the top and bottom of the spars is now less than the theoretical.

4.5. *Combined Loading Effects (Case 2).*—Although the experimental results of this case have been included in Figs. 9 to 11, no comment has been made in view of their general unreliability.

5. *Conclusions.*—5.1. The stress distribution, on a wing structure, imposed by an overhanging engine load, is considerably changed, leading to higher stress concentrations, by the shear distortion of the cross-section. The term concentration as used here denotes the local increase of stress above that predicted by the simple engineers' theory of bending.

5.2. For a structure with stiff ribs, the effect of equal up and down loads applied to the front and rear spars at one section on the stress pattern prevailing from a load at the tip, is to give concentrations appreciably greater, of the order of 20 to 30 per cent, than those calculated[1] at the loaded section. The rate of die away is, however, also greater and concentrations fall rapidly, within a distance equal to two spar depths, to below the theoretical.

Indications point to the fact that if the torque had been applied as a uniform shear per inch all around the section the concentrations would have been everywhere below the theoretical[1] (or at the most equal to the theoretical at the engine frame), the observed increase at the loaded section being due, mainly, to the local effects of an abrupt change of shear.

5.3. For a structure with flexible ribs, under similar loading conditions, the stress concentrations are considerably increased and can be as much as 100 to 150 per cent greater than the theoretical[1].

The results indicate that the concentrations would still be considerably above those calculated even if the torque were applied as a 'Batho' distribution.

5.4. An abrupt change of shear at the engine nacelle, applied by equal loads at front and rear spars, leads to stress concentrations, at the spars, on the general stress pattern. These can be increased by as much as 50 per cent at the loaded section due to rib flexibility. Taylor's theory gives an approximation to the mean of the stress concentration across any section although experimental results differ widely from the mean, being at a peak on the spars and reversing in sign at the centre of the section. The theoretical[2] rate of die away along the spars is much greater than that found experimentally.

5.5. For the case of the combined loading considered here, with the particular geometrical features of the engine loading frame, the local abrupt change of shear at the spars is much less than that under the so-called pure torsion case. In practice this means that the maximum stress concentrations produced by overhanging engine loads will not exceed those calculated by Williams's theory by as much as suggested in 5.3. The figures, 100 to 150 per cent, quoted there are reduced to approximately 70 per cent whilst for the stiff-rib model the maximum increase is of the order of 20 per cent, *i.e.*, at the lower end of the range quoted in 5.2. It should be emphasized that these figures are increases of the theoretical concentrations which may themselves be of a small order.

REFERENCES

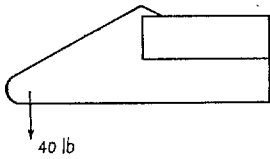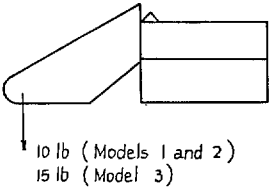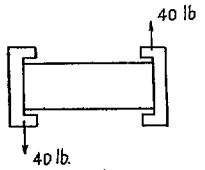| No.	Author				Title, etc.
1	D. Williams	..	..	..	The stresses in certain tubes of rectangular cross-section under torque. R. & M. 1761. May, 1936.
2	J. Taylor	..	..	..	Stresses in built-up beams due to an abrupt change of shear at a loading section. R. & M. 2775. August, 1949.
3	D. Williams and C. B. Smith	..			The experimental determination of the bending actions induced by axial end constraints in a rectangular tube in torsion. R. & M. 1775. November, 1936.
4	J. Taylor	..	..	..	The investigation of design problems on major structural components by means of static strain measurements. R. & M. 2129. November, 1945.

TABLE 1

Measurement of Rib Stiffness

Case number	Loading conditions	Relative rotation of the rear spar to the bottom surface at the first rib outboard of engine loading frame		
		Model 1	Model 2	Model 3
1	40 lb	0·93	0·94	0·97
2	10 lb (Models 1 and 2) 15 lb (Model 3)	0·92	0·95	0·76
3	40 lb / 40 lb	0·82	0·85	1·01

TABLE 2

Percentage concentrations

Gauges 1–22

Plotting symbol—Figs. 9, 10, 11							×				+				△							
Plotting symbol Figs. 5, 6, 7, 8	×	△	×			△	×			△	×			△	×			△	×	△	×	△
Model / Case / Gauge number	1	2	3	4	5	6	7	8	9	10	11	12	13	14	15	16	17	18	19	20	21	22
M1 C1	−4·19	+1·08	+0·28	—	—	−1·50	+ 5·70			− 2·53	+11·15	+ 5·41	−1·30	− 7·79	+ 8·83	0	−2·92	−2·41	+1·65	0	0	0
M2 C1	+0·94	−0·71	+4·96	—	—	−3·40	+14·32	—	—	− 7·99	+13·20	+ 6·67	−3·0	− 9·50	+ 8·60	+1·30	−2·10	−4·80	+3·35	−0·92	0	0
M3 C1	+2·20	+0·64	+2·86	—	—	−2·31	+ 7·64	+4·15	−2·10	− 5·86	+10·81	+ 3·34	−2·46	− 6·36	+ 6·93	+0·86	−1·74	−2·94	+2·17	−1·07	—	−1·19
M1 C2				—	—		+ 2·98	—	—	+ 2·06	+ 4·31	+11·95	+5·29	+ 5·95								
M2 C2				—	—		+11·90	—	—	+ 0·49	+ 6·53	+12·88	+3·80	0								
M3 C2		·		—	—		+ 4·55	+7·00	0	− 3·29	+ 6·54	+ 5·91	+0·5	− 3·93								
M1 C3	−2·38	+4·26	0	—	—	0	+ 8·57	—	—	− 4·97	+22·93	+ 5·66	−3·61	−25·13	+ 6·05	+2·91	−2·28	−5·68	−1·48	+3·32	0	+4·96
M2 C3	−0·59	+1·55	+7·12	—	—	−5·65	+20·1	—	—	−18·05	+20·78	+ 6·42	−5·27	−28·92	+10·48	+3·44	−2·47	−8·05	−0·97	+1·25	−2·25	+2·14
M3 C3	+0·24	−0·061	+2·26	—	—	−1·94	+11·41	+2·59	−2·14	−10·58	+12·14	+ 2·67	−2·25	−11·35	+ 2·90	+1·57	−0·80	−3·22	+0·65	−1·19	—	0
M1 C4	+2·28	+2·29	+0·53	—	—	+0·20	− 2·54	—	—	− 1·76	− 4·19	+ 1·58	+1·53	− 4·35	− 1·81	+1·05	+1·30	−1·60	—	0	0	0
M2 C4	+2·52	+2·92	−0·92	—	—	−1·86	− 5·63	—	—	− 8·19	− 3·29	+ 1·20	+1·50	− 4·34	− 2·29	+1·28	+1·17	−1·96	−1·17	−0·56	0	0
M3 C4	−1·37	−1·49	−1·66	—	—	−2·17	− 3·06	+0·87	+0·85	− 4·40	− 2·68	+ 1·24	+1·19	− 1·88	− 1·64	+1·41	+1·39	−1·68	−0·12	−0·14	—	+0·12

Gauges 23–44

| Plotting symbol—Figs. 9, 10, 11							×				+				△							
Plotting symbol Figs. 5, 6, 7, 8	+	□	+			□	+			□	+			□	+			□	+	□	+	□
Model / Case / Gauge number	23	24	25	26	27	28	29	30	31	32	33	34	35	36	37	38	39	40	41	42	43	44
M1 C1	−1·77	+1·86	+4·78	—	—	−1·74	+ 9·35	—	—	− 1·88	+13·46	− 5·56	−2·72	− 5·12	+ 6·68	+1·79	−2·09	−3·78	0	−0·29	−1·04	0
M2 C1	+2·64	−0·86	+8·29	—	—	−3·57	+17·55	—	—	− 5·01	+15·34	+ 2·05	−3·98	− 4·48	+ 9·10	+1·82	−2·29	−2·88	+3·38	−0·59	+1·31	+0·94
M3 C1	+2·46	+2·34	+6·57	—	—	−1·45	+12·10	−0·92	−2·73	− 4·19	+10·00	+ 2·04	−2·27	− 2·66	+ 5·29	+1·09	−1·57	−2·08	+1·61	−1·54	+0·47	+0·25
M1 C2				—	—			—	—	− 1·04	+17·34	− 3·85	−0·81	0								
M2 C2				—	—		+10·93	—	—	− 1·91	+10·42	+ 7·52	−0·71	− 1·08								
M3 C2				—	—		+ 9·52	+4·51	+0·23	− 2·55	+ 5·81	+ 3·89	−1·07	− 2·09								
M1 C3	−3·77	+3·17	+1·33	—	—	0	+ 6·44	—	—	− 4·03	+17·40	− 1·46	−4·53	−21·59	+ 5·15	+1·76	−3·79	−7·23	−2·76	+1·33	−1·72	0
M2 C3	0	0	+5·86	—	—	−6·95	+19·13	—	—	−20·05	+16·03	+ 3·36	−6·12	—	—	+1·96	−2·84	−8·92	−1·03	0	−2·79	+1·91
M3 C3	0	0	+2·57	—	—	−2·75	+11·75	+2·53	−1·54	−14·75	+ 8·67	+ 2·29	−2·15	−12·91	+ 2·71	+1·01	−1·33	−3·62	+0·80	−0·75	—	−0·12
M1 C4	+2·32	+1·96	+0·54	—	—	+0·28	− 1·92	—	—	− 1·29	− 4·68	+ 6·05	+1·30	− 4·79	− 2·02	+0·81	+0·98	−1·84	−0·16	−0·51	−0·34	+0·54
M2 C4	+0·53	−0·73	−1·65	—	—	−2·67	− 6·22	—	—	− 6·10	− 4·90	+ 0·57	+1·01	—	—	+0·24	+0·39	−2·87	−0·23	−1·08	−0·50	—
M3 C4	−1·37	−1·54	−2·49	—	—	−2·47	− 4·31	+0·82	+0·97	− 5·13	− 3·73	+ 1·02	+0·94	− 3·03	− 2·31	+1·23	+1·50	−2·10	−0·45	−0·36	−0·17	−0·21
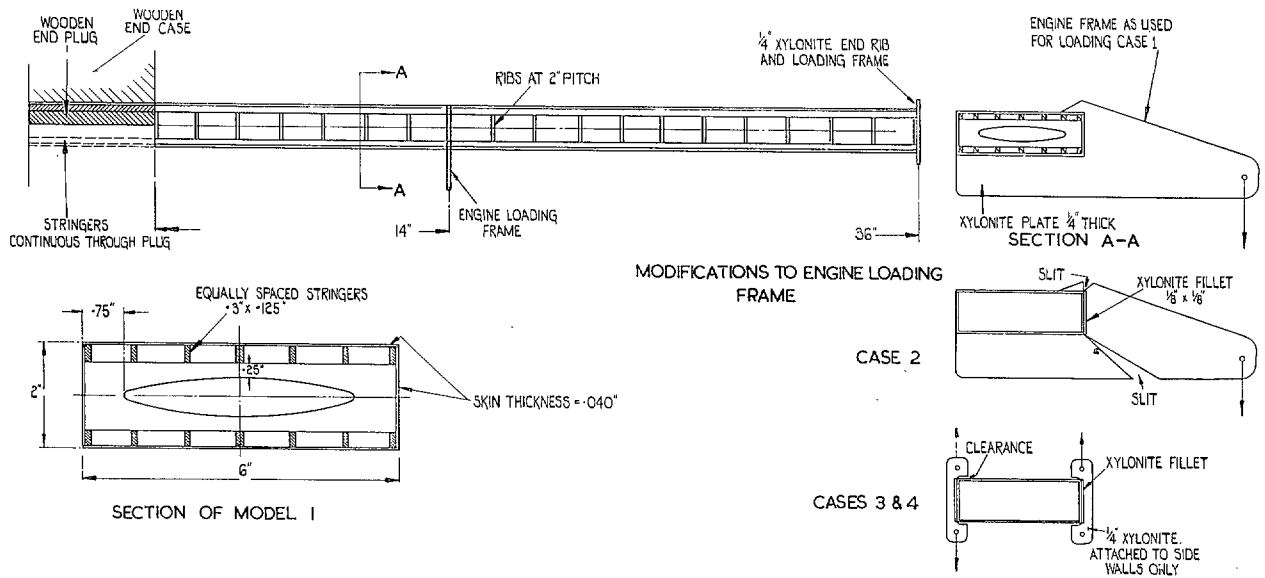
FIG. 1. General arrangement of models.
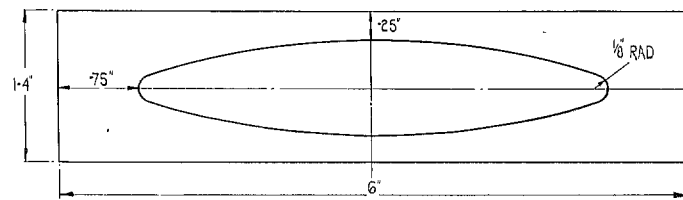
MODEL 1 ·125" THICK
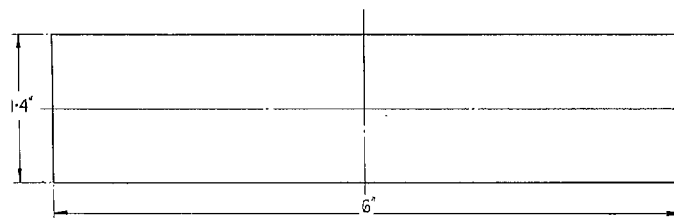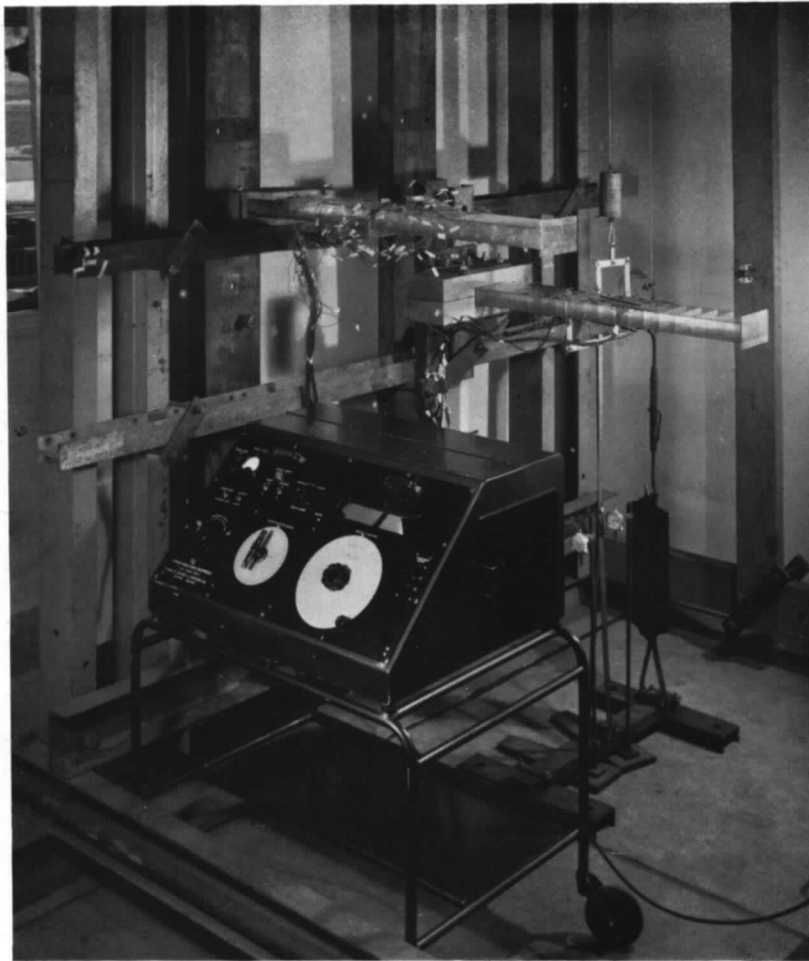
MODEL 2 ·040" THICK
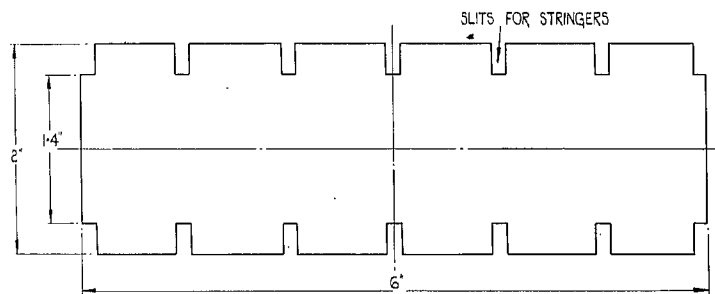
MODEL 3 ·040" THICK

FIG. 2. Ribs for each model.

10

FIG. 3.　Model 3 rigged for pure torsion test.
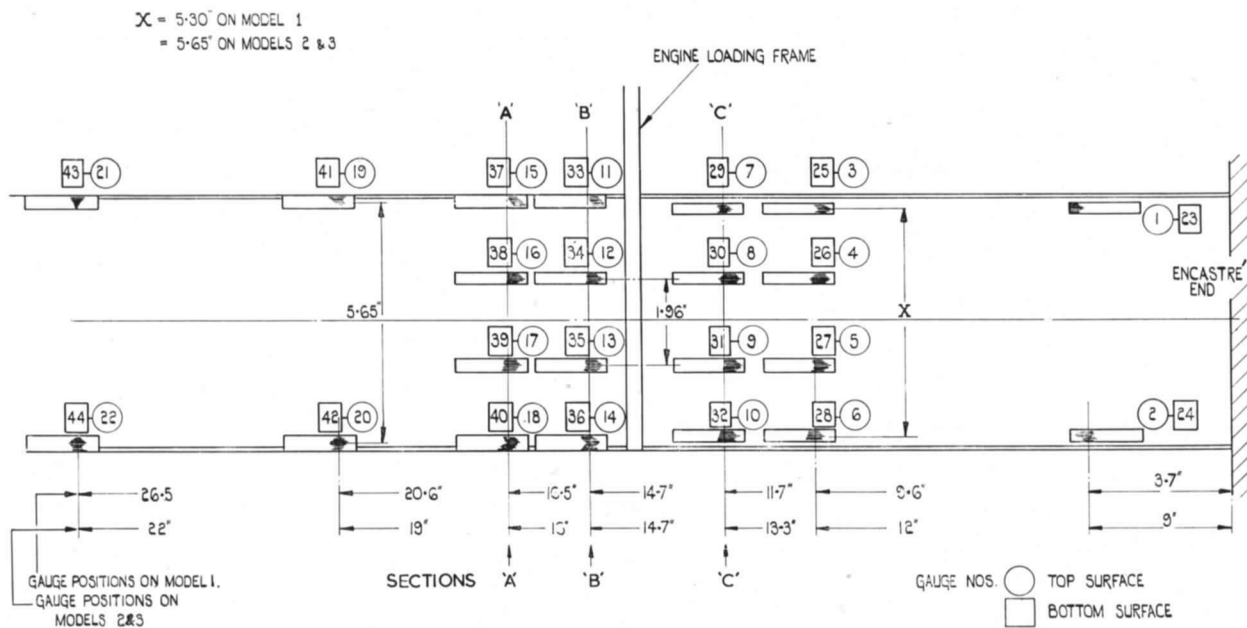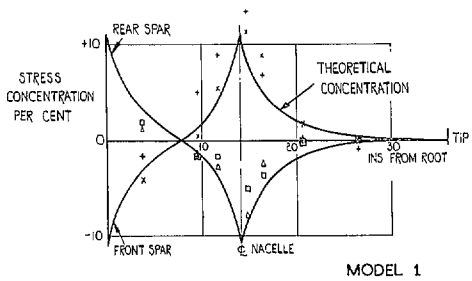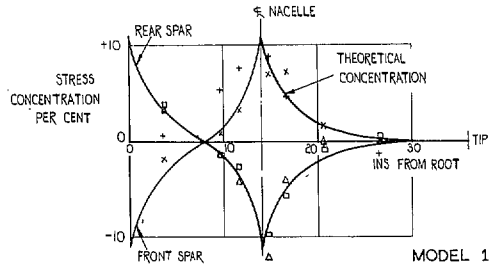

X = 5·30˝ ON MODEL 1
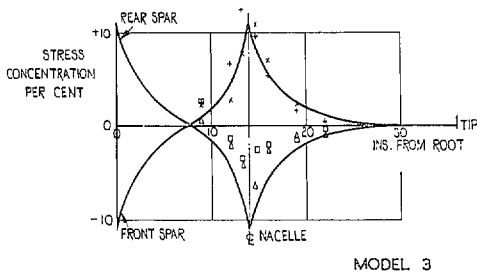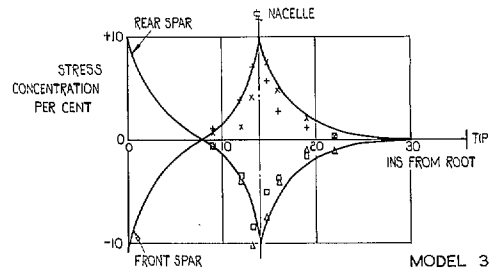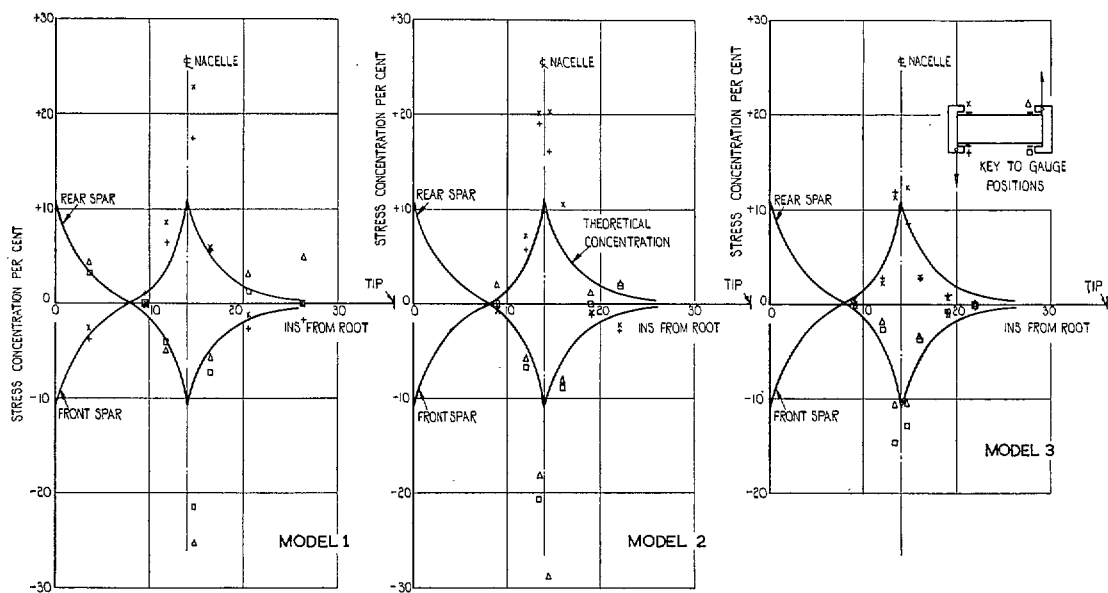 = 5·65˝ ON MODELS 2 & 3

ENGINE LOADING FRAME

FIG. 4.　Key to strain-gauge positions.

11
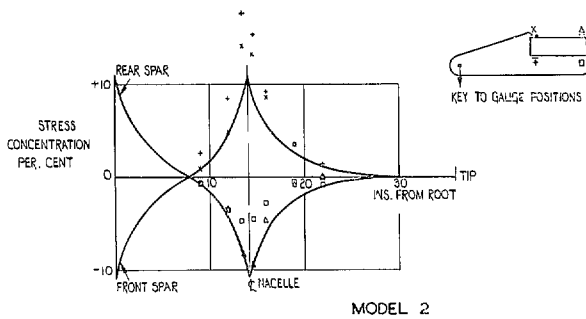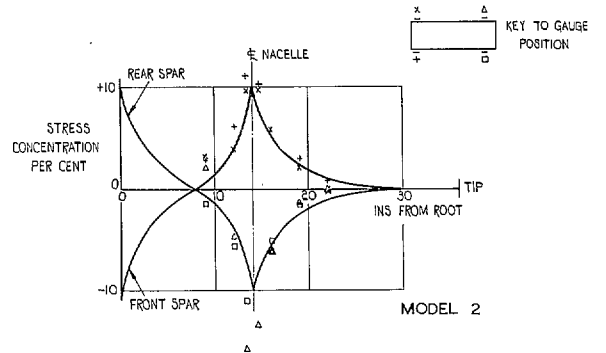
FIG. 5. Comparison of experimental results with theoretical concentrations under loading Case 1.

FIG. 6. Comparison of theoretical concentrations with experimental results obtained as a combination of loading Cases 1 and 4, *i.e.*, approximation to pure torque.

12

FIG. 7.   Comparison of experimental results with theoretical concentrations under loading Case 3.
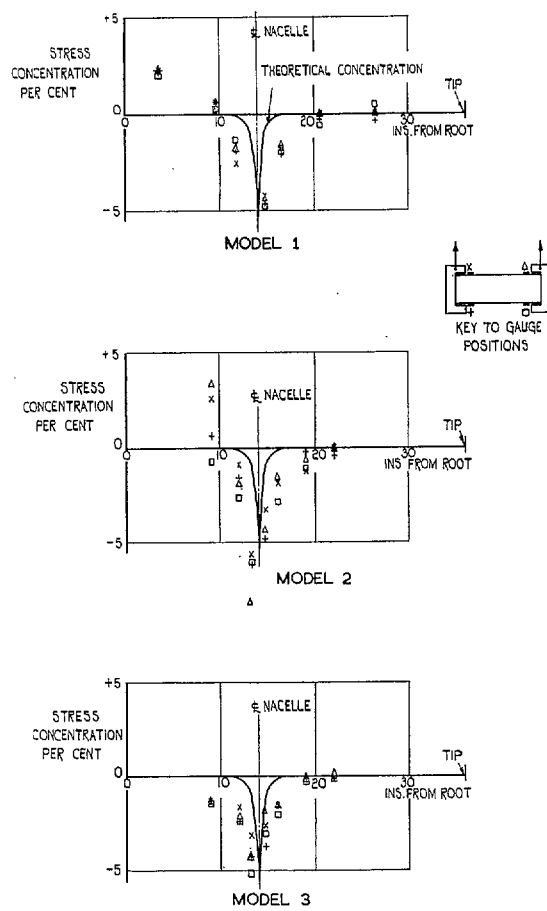
FIG. 8.   Comparison of experimental results with theoretical concentrations under abrupt change of shear (loading Case 4).

13
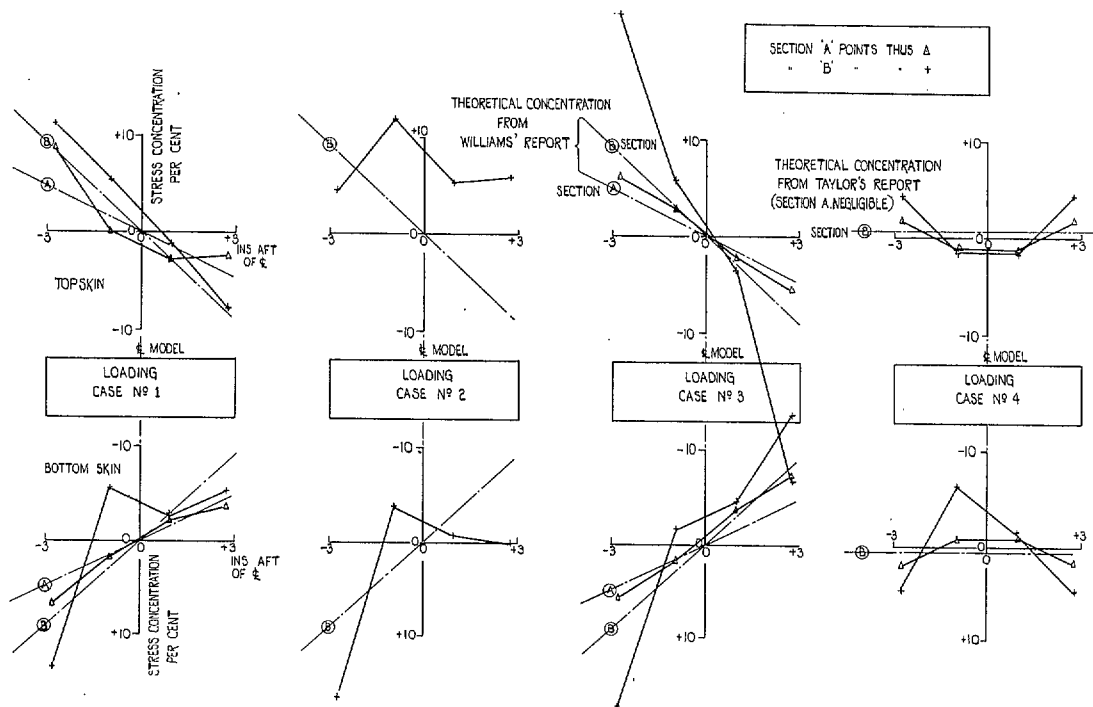
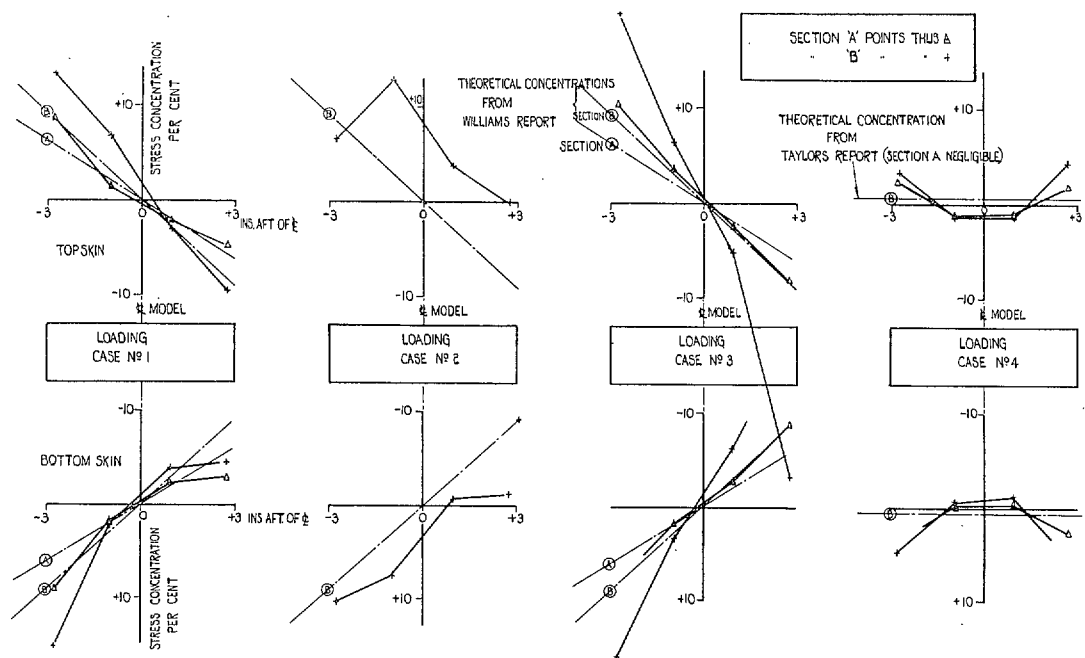FIG. 9. Stress concentrations across sections ' A ' and ' B ' (*see* FIG. 4) for Model 1.

FIG. 10. Stress concentrations across sections ' A ' and ' B ' (*see* FIG. 4) for Model 2.

14

SECTION 'A' POINTS THUS △
   "   'B'   "   "   +
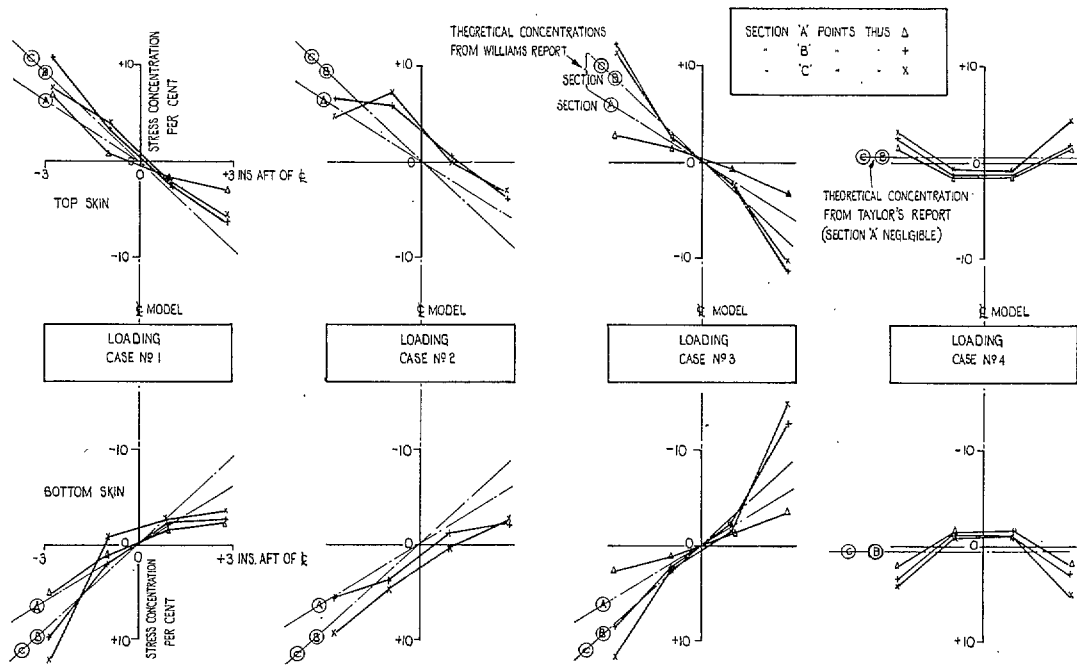   "   'C'   "   "   ×

FIG. 11.   Stress concentrations across sections ' A ', ' B ' and ' C ' (see FIG. 4) for model 3.
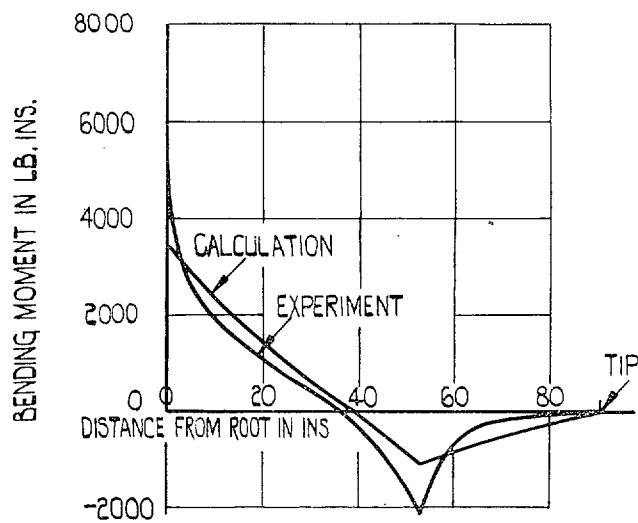

FIG. 12.   Extract from R. & M. 1775.

Publication of the

Aeronautical Research Council

ANNUAL TECHNICAL REPORTS OF THE AERONAUTICAL RESEARCH COUNCIL (BOUND VOLUMES)

1939 Vol. I. Aerodynamics General, Performance, Airscrews, Engines. 50s. (51s. 9d.).
Vol. II. Stability and Control, Flutter and Vibration, Instruments, Structures, Seaplanes, etc. 63s. (64s. 9d.)

1940 Aero and Hydrodynamics, Aerofoils, Airscrews, Engines, Flutter, Icing, Stability and Control Structures, and a miscellaneous section. 50s. (51s. 9d.)

1941 Aero and Hydrodynamics, Aerofoils, Airscrews, Engines, Flutter, Stability and Control Structures. 63s. (64s. 9d.)

1942 Vol. I. Aero and Hydrodynamics, Aerofoils, Airscrews, Engines. 75s. (76s. 9d.)
Vol. II. Noise, Parachutes, Stability and Control, Structures, Vibration, Wind Tunnels. 47s. 6d. (49s. 3d.)

1943 Vol. I. Aerodynamics, Aerofoils, Airscrews. 80s. (81s. 9d.)
Vol. II. Engines, Flutter, Materials, Parachutes, Performance, Stability and Control, Structures. 90s. (92s. 6d.)

1944 Vol. I. Aero and Hydrodynamics, Aerofoils, Aircraft, Airscrews, Controls. 84s. (86s. 3d.)
Vol. II. Flutter and Vibration, Materials, Miscellaneous, Navigation, Parachutes, Performance, Plates and Panels, Stability, Structures, Test Equipment, Wind Tunnels. 84s. (86s. 3d.)

1945 Vol. I. Aero and Hydrodynamics, Aerofoils. 130s. (132s. 6d.)
Vol. II. Aircraft, Airscrews, Controls. 130s. (132s. 6d.)
Vol. III. Flutter and Vibration, Instruments, Miscellaneous, Parachutes, Plates and Panels, Propulsion. 130s. (132s. 3d.)
Vol. IV. Stability, Structures, Wind Tunnels, Wind Tunnel Technique. 130s. (132s. 3d.)

Annual Reports of the Aeronautical Research Council—
1937 2s. (2s. 2d.)　　1938 1s. 6d. (1s. 8d.)　　1939-48 3s. (3s. 3d.)

Index to all Reports and Memoranda published in the Annual Technical Reports, and separately—
April, 1950　-　-　-　-　R. & M. 2600　2s. 6d. (2s. 8d.)

Author Index to all Reports and Memoranda of the Aeronautical Research Council—
1909—January, 1954　　　R. & M. No. 2570　15s. (15s. 6d.)

Indexes to the Technical Reports of the Aeronautical Research Council—
December 1, 1936—June 30, 1939　　R. & M. No. 1850　1s. 3d. (1s. 5d.)
July 1, 1939–June 30, 1945　　　　R. & M. No. 1950　1s. (1s. 2d.)
July 1, 1945—June 30, 1946　　　　R. & M. No. 2050　1s. (1s. 2d.)
July 1, 1946—December 31, 1946　　R. & M. No. 2150　1s. 3d. (1s. 5d.)
January 1, 1947—June 30, 1947　　　R. & M. No. 2250　1s. 3d. (1s. 5d.)

Published Reports and Memoranda of the Aeronautical Research Council—
Between Nos. 2251–2349　　　　R. & M. No. 2350　1s. 9d. (1s. 11d.)
Between Nos. 2351–2449　　　　R. & M. No. 2450　2s. (2s. 2d.)
Between Nos. 2451–2549　　　　R. & M. No. 2550　2s. 6d. (2s. 8d.)
Between Nos. 2551–2649　　　　R. & M. No. 2650　2s. 6d. (2s. 8d.)